Supporting Information

A Processable, Scalable, and Stable Full-Color Ultralong Afterglow System Based on Heteroatom-Free Hydrocarbons Doped Polymers

Xiaoxin Zheng, Quanxiang Han, Qinglian Lin, Cuicui Li, Jinke Jiang, Qing Guo, Xin Ye, Wang Zhang Yuan, Yang Liu, and Xutang Tao**

X. X. Zheng, Q. X. Han, Q. L. Lin, C. C. Li, J. K. Jiang, Dr. Q. Guo, Dr. X. Ye, Prof. Y. Liu and Prof. X. T. Tao
State Key Laboratory of Crystal Materials, Institute of Crystal Materials, Shandong University, Jinan 250100, PR China
E-mail: liuyangicm@sdu.edu.cn, and txt@sdu.edu.cn

Prof. W. Z. Yuan
School of Chemistry and Chemical Engineering, Frontiers Science Center for Transformative Molecules, Shanghai Key Lab of Electrical Insulation and Thermal Aging, Shanghai Jiao Tong University, Shanghai, 200240, China

Characterization

^{1}H NMR spectra and ^{13}C NMR spectra were recorded on a 400 MHz Bruker AVANCE III spectrometer. Element analysis was carried out by an Element Vario EL Cube element analyzer. MALDI-TOF-MS analysis was measured on a Bruker ultrafleXtreme MALDI-TOF/TOF. UV-vis spectra were measured on a Shimadzu UV-2600. Powder X-ray diffraction (PXRD) was performed on a Bruker D8 ADVANCE X-ray diffractometer. The single-crystal X-ray diffraction data were collected on a Bruker SMART APEX II CCD area detector of a D8 goniometer at 298 K. Fluorescence, phosphorescence spectra, and phosphorescence lifetime were measured by Edinburgh Instruments FLS980 fluorescence spectrometer with a Xe lamp as the excitation source. The total quantum yield was measured by the matching integrating sphere. The phosphorescence quantum yield was calculated according to the following formula:

$$\Phi_{phos} = \frac{B}{A} \times \Phi_{PL}$$

In the formula, A, B, and Φ are the integrated area of the total luminescence spectrum and phosphorescence spectrum, the total quantum yield, and the phosphorescence quantum yield. The fluorescence lifetime is measured using EPL-375/EPLED-300 laser as the excitation light source. In the photoactive process, the excitation light (365 nm and 254 nm) intensity used in this study was 300 mW/cm^2.

Theoretical calculation

Using the Gaussian program, these three molecules were optimized with dispersion corrected density functional theory (DFT-D3) at the PBE0-D3/def2-SVP level. In order to investigate the photophysical properties of these molecules, the excited electronic structures were calculated at the PBE0-D3/def2-TZVP level with the time-dependent density functional theory (TDDFT) method. The natural transition orbits (NTOs) and the contributions of molecular orbital transitions were obtained by electron excitation analysis from the transition density matrix of TD-DFT calculation using the Multiwfn program [1] The spin-orbit coupling (SOC) matrix elements were calculated using the spin-orbit mean-field (SOME) methods based on the excited-state wave functions obtained from TDDFT calculations. These calculations were performed using ORCA 4.2.1 program [2, 3]

Reagents and materials

The poly(methyl methacrylate) (PMMA, No defined molecular weight, Product No. M0088, 2.0 to 4.0 mPa*s(10 mg/mL THF, 20 ℃)), 1-indanone, and hexaphenylbenzene obtained from Tokyo Chemical Industry (TCI). The polycarbonate (PC, average Mw ~26,000 by GPC) was purchased from Macklin Inc. Unless otherwise stated, all chemicals and reagents were used as received from chemical companies without any further purification.

Synthesis

Compounds truxene and hexabenzocoronene were synthesized as below. [4]

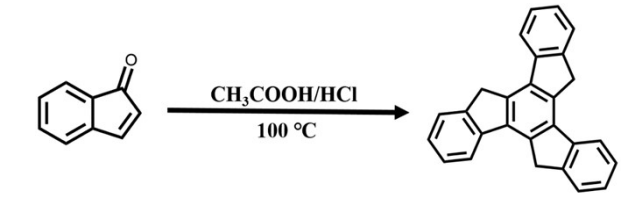

1-Indanone **Truxene**

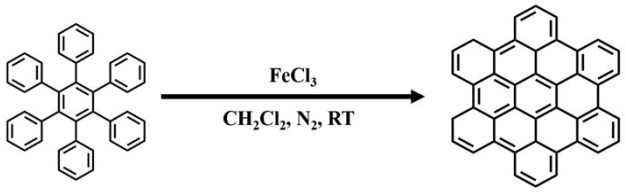

Hexaphenylbenzene **Hexabenzocoronene**

Truxene: 1-indanone (13.2 g 100 mmol) was added to the mixture of acetic and concentrated aqueous hydrochloric acids (2:1), then the solution was stirred at 100 °C for 16 hours. When the cooled solution was poured into ice water, the precipitate was obtained. The solid precipitate was washed with water and acetone to give a white powder with a 98% yield. ^{1}H NMR (400 MHz, $CDCl_3$) δ: 7.91 (d, 3H), 7.65 (d, 3H), 7.46 (t, 3H), 7.35 (t, 3H), 4.22 (s, 6H). ^{13}C NMR (125 MHz, $CDCl_3$) δ: 142.78, 140.68, 136.08, 134.17, 125.91, 125.28, 124.12, 120.87, 35.53. MALDI-TOF-MS (m/z): 342.137, calc. 342.14. Elemental analysis calculated for $C_{27}H_{18}$ (%): C 94.70, H 5.30;

found (%): C 94.60, H 5.16.

Hexabenzocoronene: 1.6 g (3 mmol) hexaphenylbenzene and 100 ml CH_2Cl_2 were put into a 250 ml flask, and the solution was agitated and bubbled with nitrogen for 30 minutes. 2.4 g $FeCl_3$ was dissolved in 10 ml degassed CH_3NO_2 before being injected dropwise into the hexaphenylbenzene solution. The reactants were stirred for 4 hours with nitrogen bubbling after the addition of $FeCl_3$. The reaction was then quenched using CH_3OH, resulting in the precipitate. The precipitate was filtered and washed with acetone, water, and hydrochloric acid (1.0 mol/L) in that order. About 1.5 g (2.85 mmol) powder was produced after vacuum drying. The yield of hexabenzocoronene is about 95%. ^{13}C NMR (15 kHz, solid) δ: 110-140. MALDI-TOF-MS (m/z): 522.062, calc. 522.14. Elemental analysis calculated for $C_{42}H_{18}$ (%): C 96.53, H 3.47; found (%): C 96.04, H 3.80.

Preparation of the RTP materials

Using CH_2Cl_2 as the solvent**,** the raw solutions of PMMA, truxene, coronene, hexabenzocoronene, and perylene red with the concentrations 200 mg/ml, 1mg/ml, 0.5mg/ml, 0.01mg/ml, and 1mg/ml, respectively were prepared.

The inks: Dissolve 2.0 mg truxene into 10 mL 200 mg/ml PMMA solution to obtain the ink of T-PMMA. Likewise, dissolve 2.0 mg coronene into 10 mL 200 mg/ml PMMA solution to obtain the ink of C-PMMA and dissolve 2.0 mg coronene and 2.0 mg perylene red into 10 mL 200 mg/ml PMMA solution to obtain the ink of P-C-PMMA.

The films: The solutions (containing 2 g PMMA and the corresponding chromophores) ratio-mixed by the raw solutions were placed in an evaporating dish with a flat bottom, then left for 48 hours to evaporate the solvent and solidify the doping systems. The photophysical properties were investigated after drying for 12 hours at 100 °C. The films can also be obtained by melt process. Mix PMMA with corresponding chromophores in molten state at 250 °C by vigorous and repeated agitation. Then put the doped PMMA into the Hot Press, and after pressing, the corresponding films can be obtained.

The fibers: The obtained doped PMMA were heated to molten and then drawn into fibers at 250 ℃.

The 3D objects: Take 25 g of newly distilled methyl methacrylate (MMA) and 30mg of BPO into a conical flask. then, gently shake the flask until all of the BPO has dissolved. The resultant mixture was heated to 60 ℃ for hours under nitrogen until it is as sticky as glycerin. Cool the reactants quickly to room temperature to stop the reaction. Then, pour the cooled reactants into the mold and continue the reaction for 24 hours at 40 ℃ under nitrogen. Finally, the reactants were treated at 100 ℃ for 3 hours. After removing the molds, various shapes of RTP 3D objects could be obtained.

Table S1. RTP properties of polymer-based materials with long-lived lifetime (>100 ms).

No.	Doped polymer		λ_{em} (nm)	τ_{Phos} (ms)	Φ_{Phos} (%)	Refs.
	polymer	chromophore				
1	PMMA	**G1**	530	208	50.0	ref[5]
2	PMMA	**G2**	541	230	3.1	ref[6]
3	PMMA	**G3**	541	230	3.9	ref[6]
4	PMMA	**G4**	564	5580	1.7	ref[7]
5	PMMA	**G5**	565	23000	12.0	ref[7b]
6	PMMA	**G6**	521	700	4.6	ref[8]
7	PMMA	**G7**	516	330	5.7	ref[8]
8	PMMA	**G8**	544	680	1.2	ref[8]
9	PMMA	**G9**	542	176	<1	ref[8]
10	PMMA	**G10**	546	600	-	ref[9]
11	PMMA	**G11**	508	500	-	ref[9]
12	PMMA	**G12**	440	900	-	ref[9]
13	PMMA	**G13**	486	600	-	ref[9]
14	PMMA	**G14**	484	1880	3.7	ref[10]
15	PMMA	**G15**	487	750	5.4	ref [10]
16	PMMA	**G16**	482	1740	5.4	ref[10]
17	PMMA	**G17**	486	2150	2.7	ref[10]
18	PMMA	**G18**	523	580	4.1	ref[11]
19	PLA	**G19**	488	581	-	ref[12]
20	PLA	**G20**	505	386	-	ref[12]
21	PLA	**G21**	504	214	-	ref[12]
22	PLA	**G22**	541	520	-	ref[12]
23	PLA	**G23**	541	424	-	ref[12]
24	PLA	**G24**	526	612	-	ref[12]
25	PLA	**G25**	520	194	-	ref[13]
26	PLA	**G26**	511	178	-	ref[13]
27	PLA	**G27**	532	340	-	ref[13]
28	PLA	**G28**	534	135	-	ref[13]
29	PLA	**G29**	531	188	-	ref[13]
30	PLA	**G30**	541	813	-	ref[14]
31	PLA	**G31**	544	341	-	ref[14]
32	PLA	**G32**	572	137	-	ref[15]
33	PLA	**G33**	557	109.7	-	ref[15]
34	PLA	**G34**	489	255	-	ref[16]
35	PLA	**G35**	543	270	-	ref[16]
36	PLA	**G36**	567	295	-	ref[16]
37	PLA	**G37**	452	113	-	ref[16]
38	PVA	**G38**	527	109.3	1.5	ref[17]
39	PVA	**G39**	519	700	27.0	ref[18]
40	PVA	**G40**	525	820	23.7	ref[18]
41	PVA	**G41**	460	1210	16.0	ref[18]

42	PVA	**G42**	420	240	2.6	ref[18]
43	PVA	**G43**	500	900	9.4	ref[18]
44	PVA	**G44**	500	200	0.5	ref[18]
45	PVA	**G45**	500	567	2.4	ref[19]
46	PVA	**G46**	501	585	4.8	ref[19]
47	PVA	**G47**	500	730	<1	ref[19]
48	PVA	**G48**	532	2460	23.4	ref[20]
49	PVA	**G49**	450	2260	17.5	ref[20b]
50	PVA	**G50**	450	72.07	36.8	ref[20b]
51	PVA	**G51**	480	750	11.2	ref[21]
52	PVA	**G52**	488	828.8	5.0	ref[22]
53	PVA	**G53**	460	190	11.9	ref[23]
54	PVA	**G54**	460	450	15.0	ref[23]
55	PVA	**G55**	460	420	5.1	ref[23]
56	PVA	**G56**	440	990	6.1	ref[24]
57	PVA	**G57**	434	1290	1.0	ref[24]
58	PAN	**G58**	487	968.1	0.6	ref[25]
59	PAN	**G59**	540	301.7	6.1	ref[25]
60	PAN	**G60**	553	245.1	2.1	ref[25]
61	PAN	**G61**	617	100.2	0.2	ref[25]
62	PVA	**G62**	463	1720	8.2	ref[26]
63	PVA	**G63**	480	1810	19.8	ref[26]
64	P(VAc-co-AA)	**G64**	470	1866	55.99	ref[27]
65	PA6	**G65**	525	747	14.7	ref[28]
66	PVA	**G66**	488	2044.86	2.8	ref[29]
67	PMMA	**G67**	530	122.44	3.47	ref[30]
68	PMMA	**G68**	~520	576.4	57.4	ref[31]
69	PMMA	**G69**	~520	589.2	56.2	ref[31]
70	PMMA	**G70**	~520	529.3	56.0	ref[31]
71	PMMA	**G71**	~520	453.7	54.9	ref[31]
72	PMMA	**G72**	~520	265.9	27.2	ref[31]
73	PMMA	**G73**	516	770	33.31	ref[32]
74	PMMA	**G74**	510	1510	42.05	ref[32]
75	PMMA	**G75**	514	250	10.02	ref[32]
76	PMMA	**G76**	530	260	18.14	ref[32]
77	PMMA	**G77**	537	1640	20.43	ref[32]
78	PMMA	**G78**	~550	406	-	ref[33]
79	PVA	**G79**	470	3290	33.1	ref[34]
No.	**Modified polymer**		**λ_{em} (nm)**	**τ_{Phos} (ms)**	**Φ_{Phos} (%)**	**Refs.**
80	**P1**		475	2430	7.51	ref[35]
81	**P2**		500/527	2160	2.26	ref[36]
82	**P3**		501/530	1830	4.03	ref[36]

83	**P4**	505/530	1700	7.52	ref[36]
84	**P5**	510/534	1990	4.30	ref[36]
85	**P6**	498	401	10.4	ref[37]
86	**P7**	480	2139	-	ref[38]
87	**P8**	500	1007	-	ref[39]
88	**P9**	509	170	-	ref[40]
89	**P10**	445/517/547	428/949/1096	23.2	ref[41]
90	**P11**	447/514	578/609	-	ref[41]
91	**P12**	396/444	150/166	1.7	ref[42]
92	**P13**	436	615	0.6	ref[42]
93	**P14**	458/486	391/576	7.6	ref[42]
94	**P15**	496	637	0.1	ref[42]
95	**P16**	505/542/580	450/577/423	0.3	ref[42]
96	**P17**	538	1039	4.3	ref[42]
97	**P18**	490/516/616/667/730	63/80/170/122/95	0.3	ref[42]
98	**P19**	414	4200	10	ref[43]
No.	**TS-FRET polymer**	**λ_{em} (nm)**	**τ_{Phos} (ms)**	**Φ_{Phos} (%)**	**Refs.**
99	**P1+F1**	533	1600	51.68	ref[35]
100	**P1+F2**	581	1900	60.88	ref[35]
101	**G48+PVA+F3**	610	1330	25.65	ref[20a]
102	**G48+PVA+F4**	560	870	52.64	ref[20a]
103	**P19+ F5**	560	1700	30.5	ref[43]
104	**P19+ F6**	502	1800	36.0	ref[43]
105	**P19+ F7**	570	1500	20.8	ref[43]
106	**P19+ F2**	620	2200	27.9	ref[43]
107	**G79+PVA+F8**	650	600	-	ref[34]
108	**G79+PVA+F2**	590	860	-	ref[34]
109	**G79+PVA+F8+F9**	810	200	0.4	ref[34]

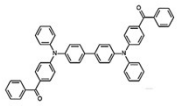

G1

G2-G3

G2

G3

G4

G5

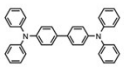

G6

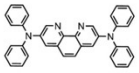

G7

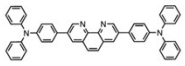

G8

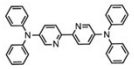

G9

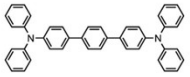

G10

G11

G12

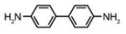

G13

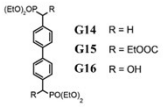

G14 R = H
G15 R = EtOOC
G16 R = OH

G14-G16

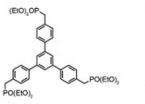

G17

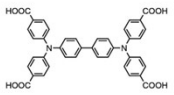

G18

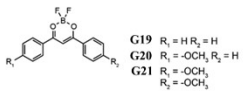

G19 R_1 = H R_2 = H
G20 R_1 = -OCH_3 R_2 = H
G21 R_1 = -OCH_3 R_2 = -OCH_3

G19-G21

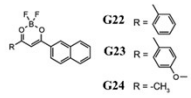

G22 R =
G23 R =
G24 R = -CH_3

G22-G24

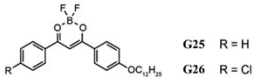

G25 R = H
G26 R = Cl

G25-G26

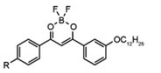

G27 R = H
G28 R = F
G29 R = Cl

G27-G29

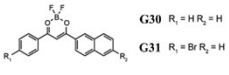

G30 R_1 = H R_2 = H
G31 R_1 = Br R_2 = H

G30-G31

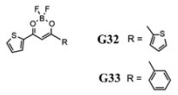

G32 R =
G33 R =

G32-G33

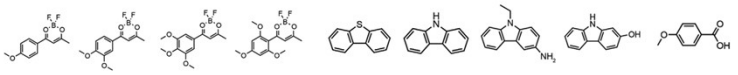

G34 G35 G36 G37 G38 G39 G40 G41 G42

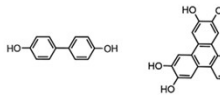

G43

G44

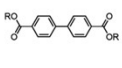

G45 R = H
G46 R = Na
G47 R = CH_3

G45-G47

G48

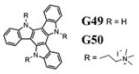

G49 R = H
G50 R =

G49-G50

G51

G52

G53

G54

G55

G56-G57

G56

G57

G58

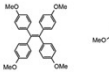

G59

G60

G61

G62

G63

G64

G65

G66

G67

G73

G74

G75

G76

G77

G68 X= H, TPMN
G69 X= F, TPMF
G70 X= Cl, TPMCl
G71 X= Br, TPMBr
G72 X= I, TPMI

G68-G72

G78

G79

P1

P2-P5

P6

P7

P8

P9

P10

P11

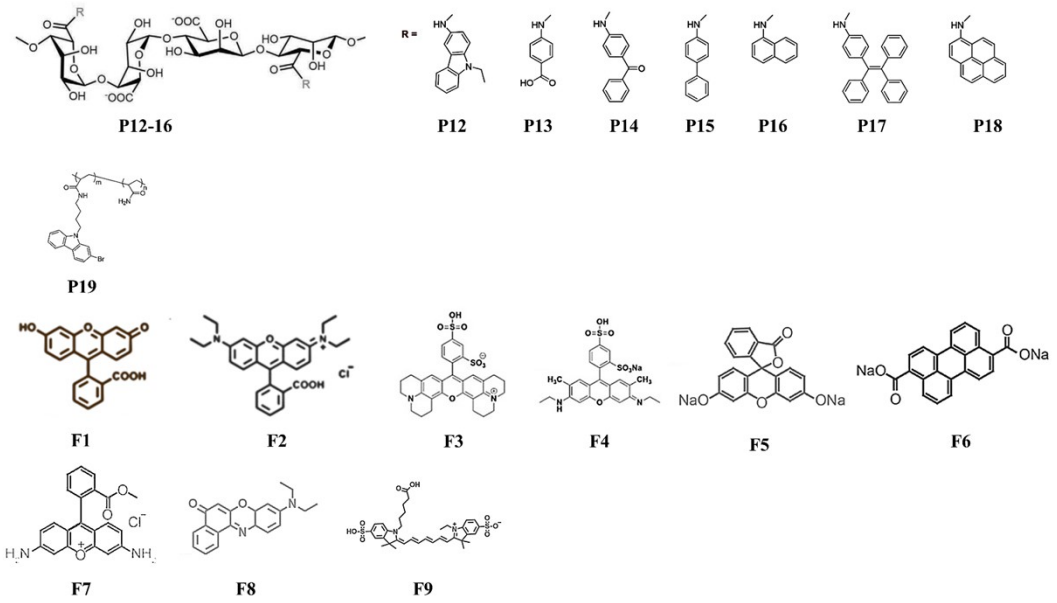

Fig. S1. Molecular structures of polymer-based materials with long-lived lifetime (>100 ms).

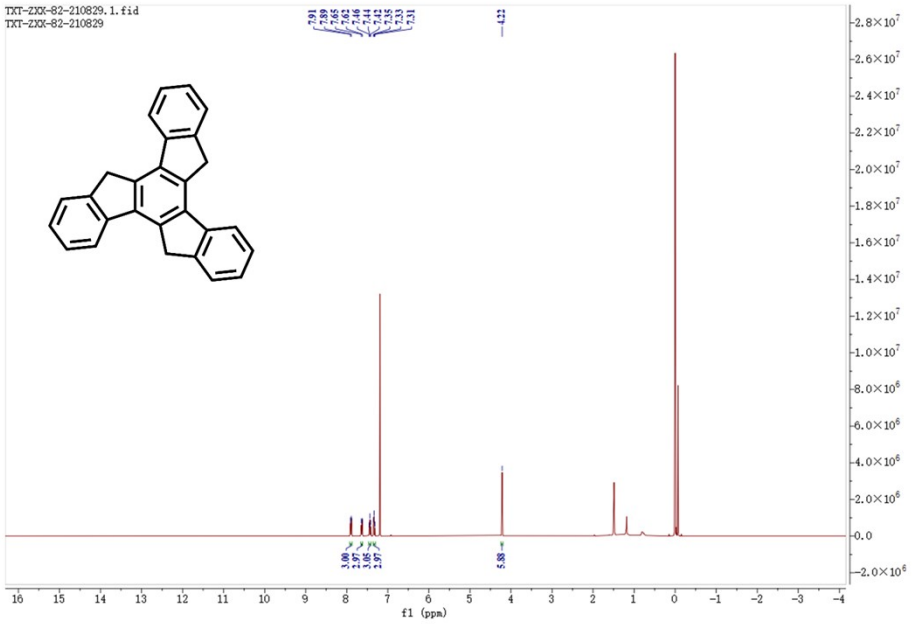

Fig. S2. ^{1}H NMR spectrum of Truxene in $CDCl_3$.

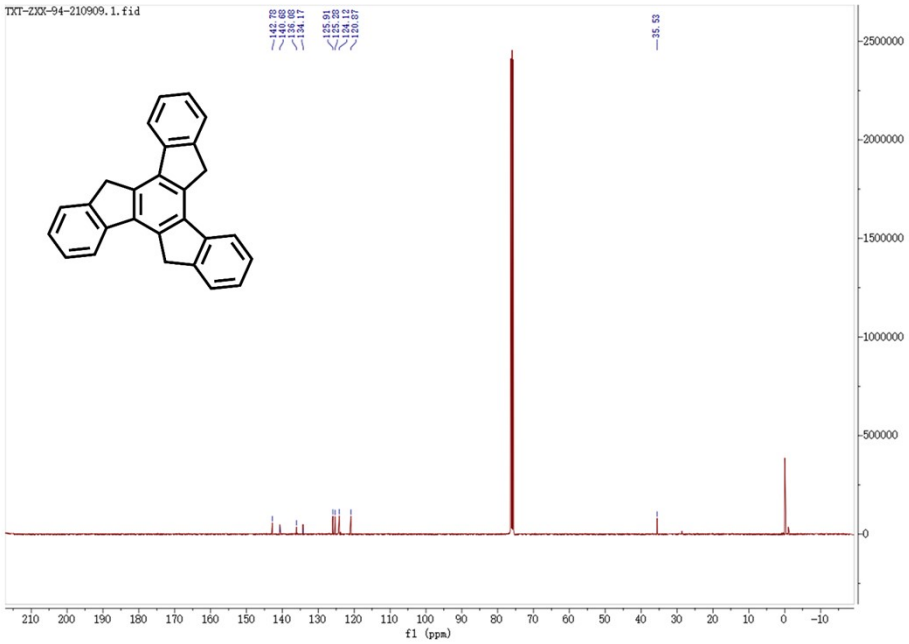

Fig. S3. ^{13}C NMR spectrum of truxene in $CDCl_3$.

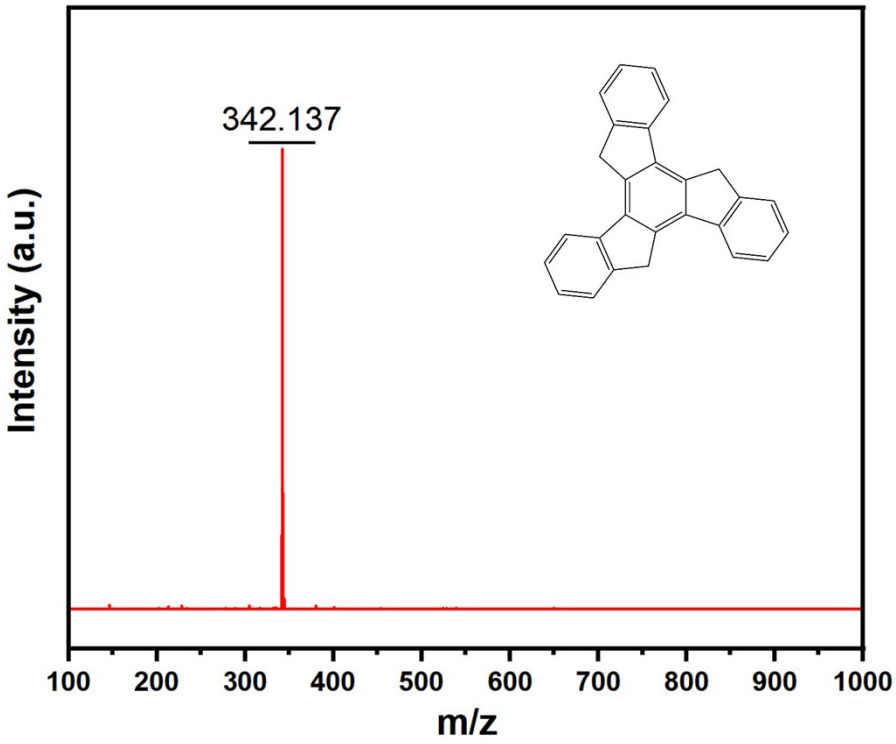

Fig. S4. MALDI-TOF-MS spectrum of truxene.

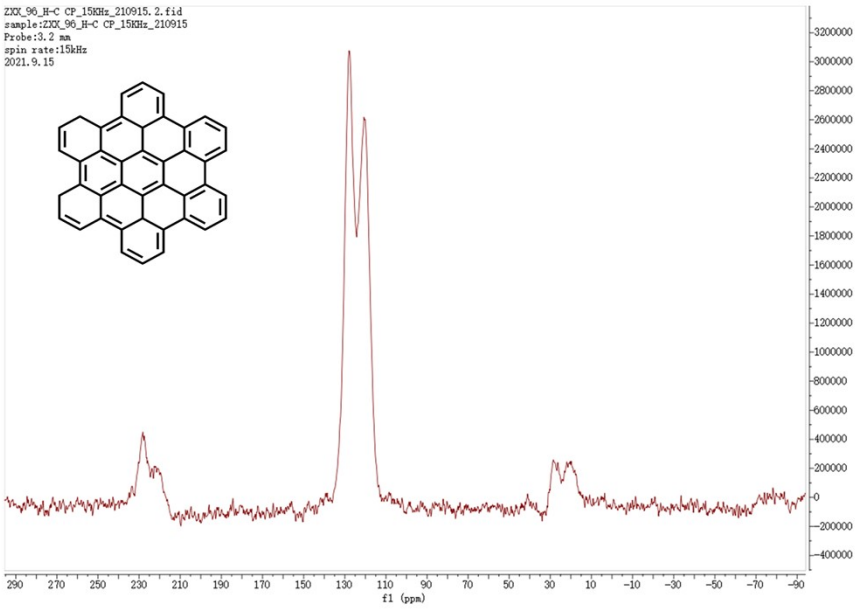

Fig. S5. ^{13}C NMR (solid) spectrum of hexabenzocoronene.

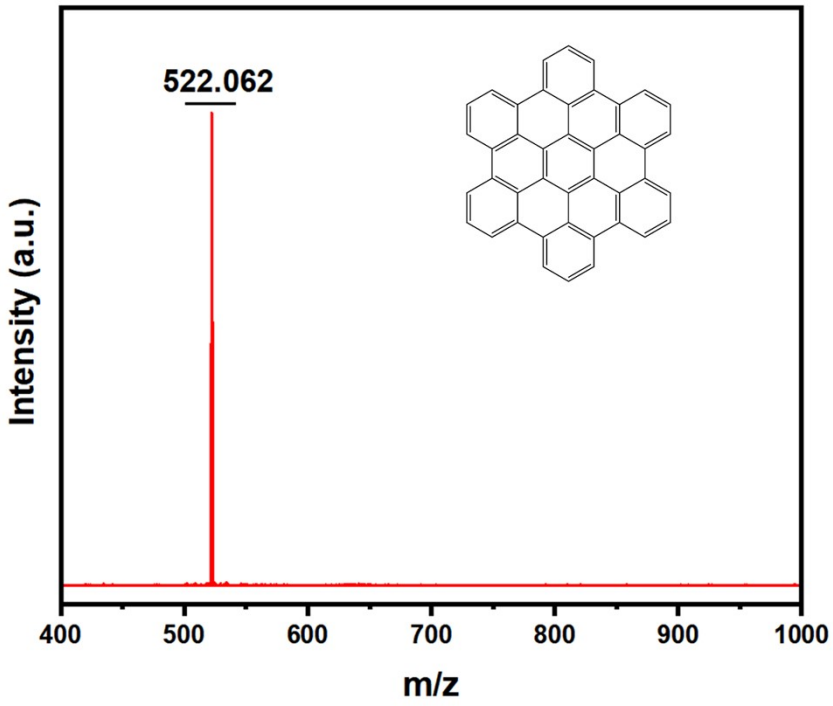

Fig. S6. MALDI-TOF-MS spectrum of hexabenzocoronene.

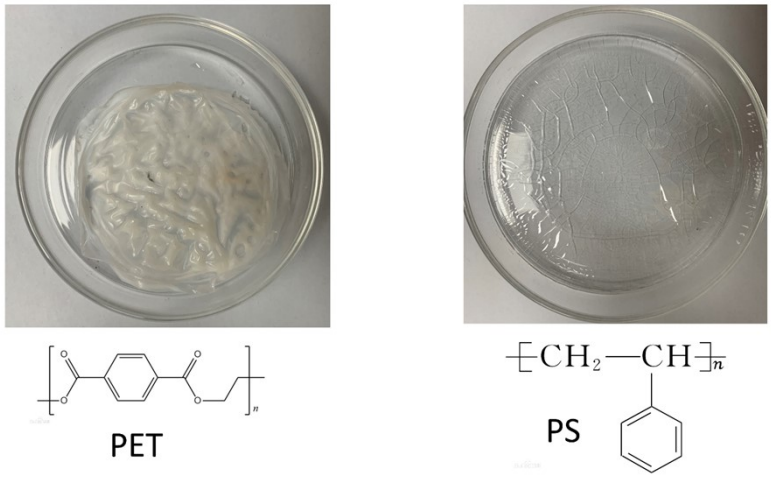

Fig. S7. The doped films of PET and PS constructed by solution method.

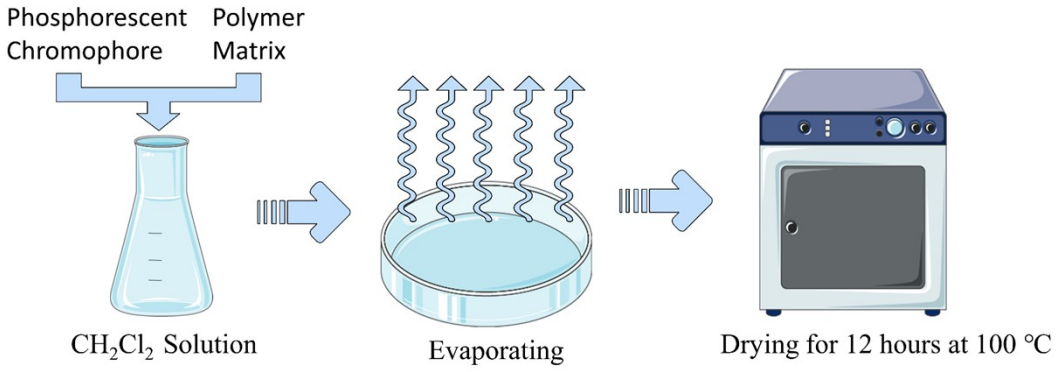

Fig. S8. Schematic illustration of the solution method for compatibility determination.

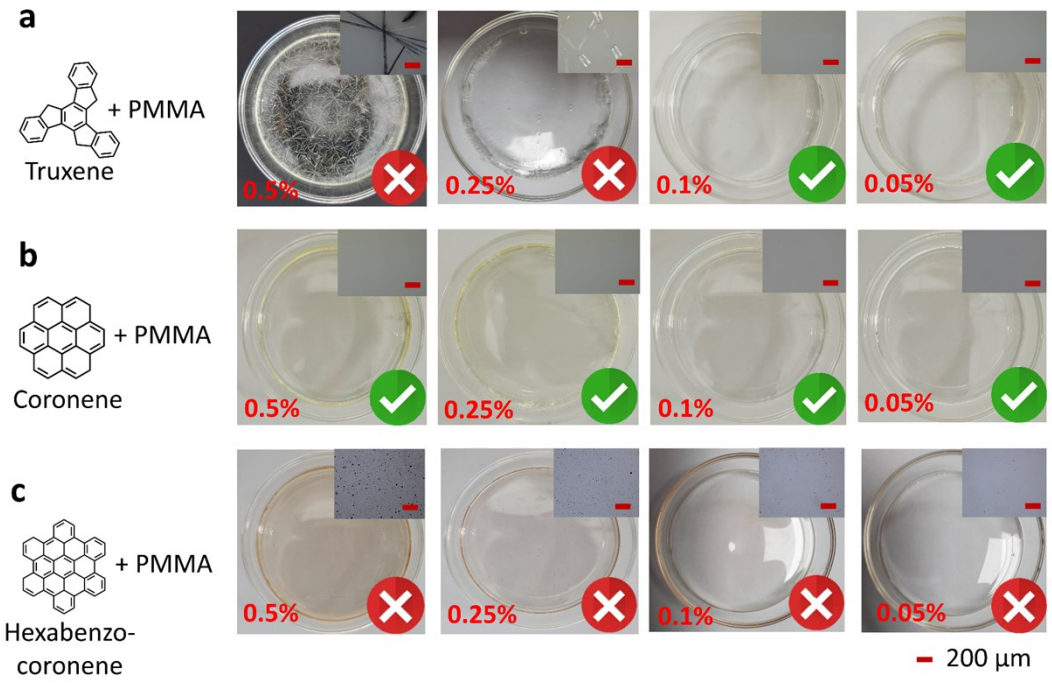

Fig. S9. The compatibility of PMMA and chromophores.

Fig. S10. The compatibility of PC and chromophores.

Table S2. The compatibility of PC/PMMA and chromophores.

	PMMA				**PC**			
	0.5%	0.25%	0.1%	0.05%	0.5%	0.25%	0.1%	0.05%

Truxene	NO	NO	YES	YES	YES	YES	YES	YES
Coronene	YES	YES	YES	YES	YES	YES	YES	YES
Hexabenzocoronene	NO	NO	NO	NO	NO	NO	YES	YES

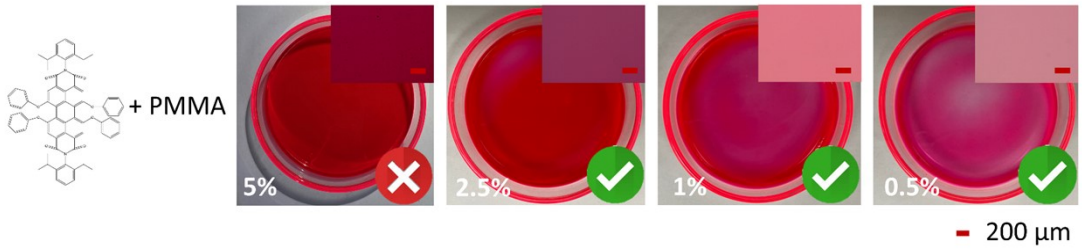

Fig. S11. The compatibility of PMMA and perylene red.

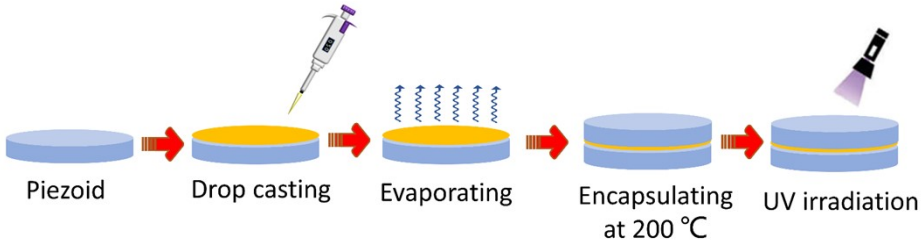

Fig. S12. Scheme of fabrication and encapsulation process of the PMMA/PC films doped with chromophore.

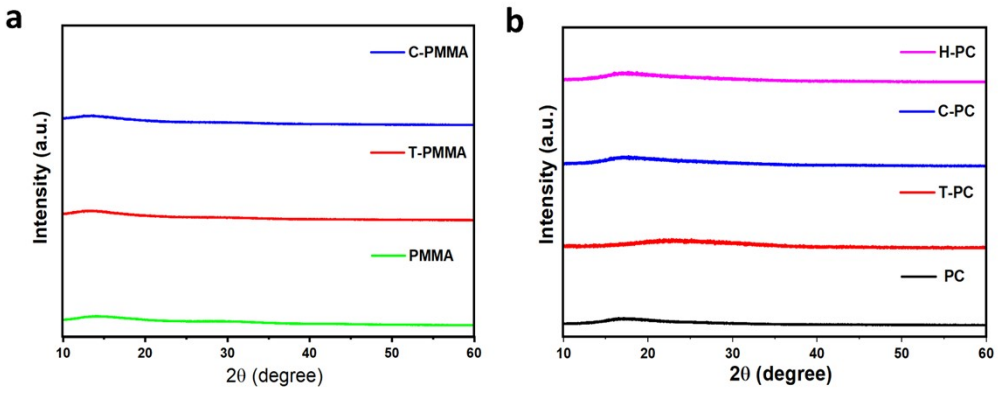

Fig. S13. The powder X-ray diffraction (PXRD) of (a) C-PMMA, T-PMMA, PMMA and (b) H-PC, C-PC, T-PC, PC.

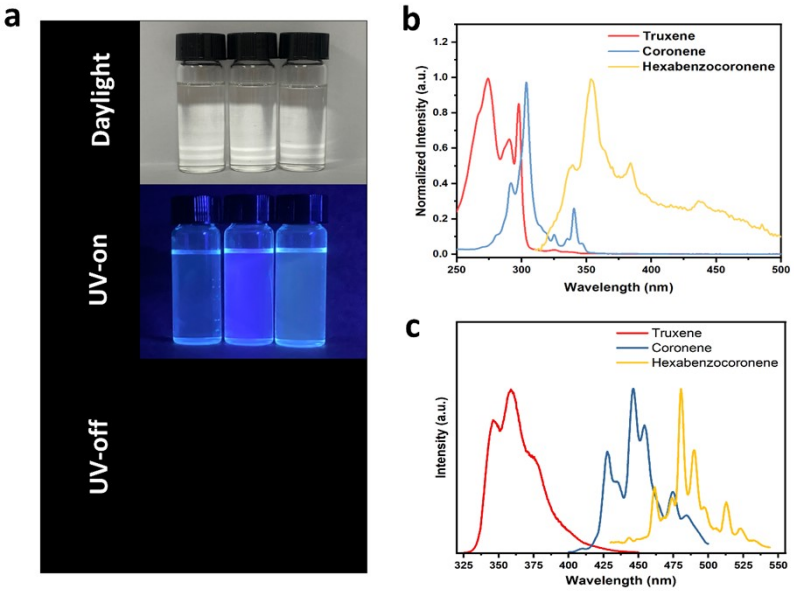

Fig. S14. (a) Photographs of the truxene, coronene and hexabenzocoronene solutions under the daylight, before and after turning off the excitation light. (b) The absorption spectra of truxene, coronene and hexabenzocoronene solutions. (c) The steady-state photoluminescence spectra of truxene, coronene and hexabenzocoronene solutions.

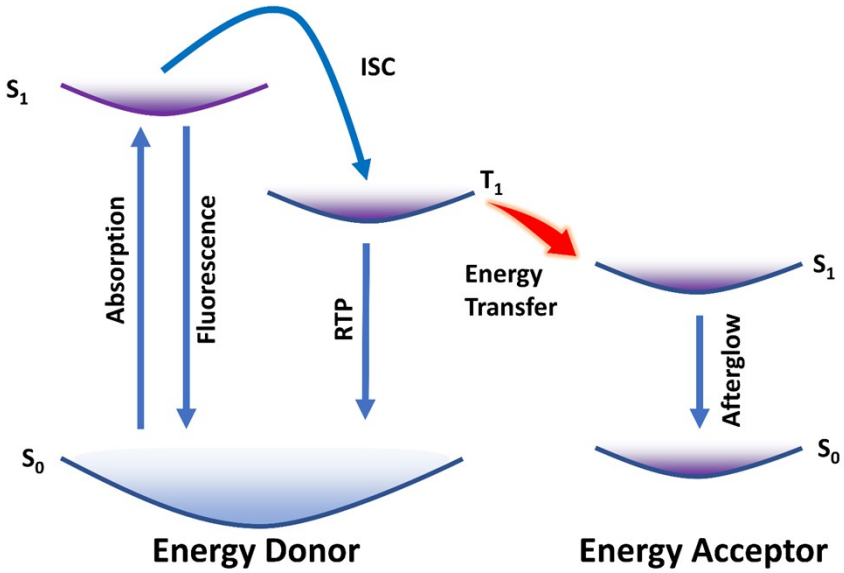

Fig. S15. Simplified Jablonski diagram to explain the phosphorescence energy transfer (ISC = intersystem crossing, RTP = room temperature phosphorescence).

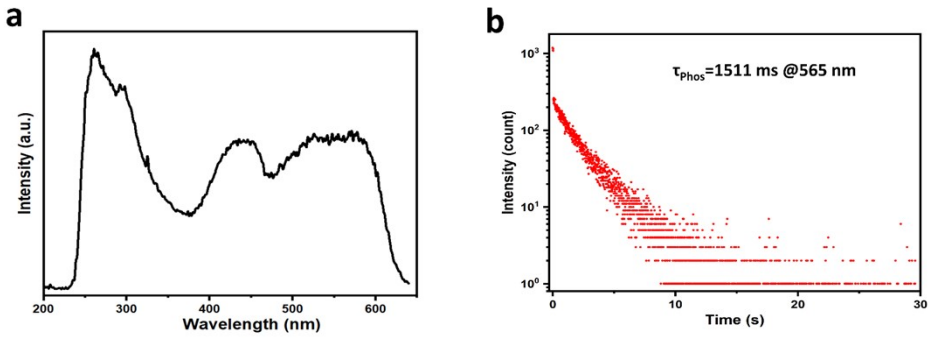

Fig. S16. (a) The excitation spectra of P-PMMA (perylene red doped PMMA, the concentration of perylene red is 0.1 wt %, λ_{em} = 650 nm). (b) Phosphorescence lifetime decay profile of P-C-PMMA at 565 nm.

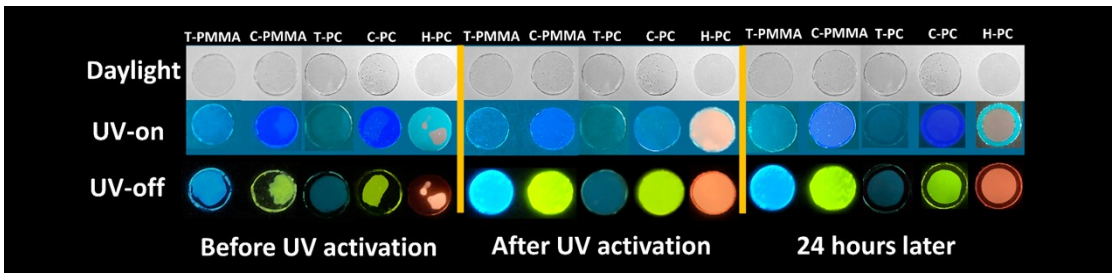

Fig. S17. Corresponding time-dependent photographs of the doped PMMA/PC films taken before UV activation/after UV activation/24 hours later process.

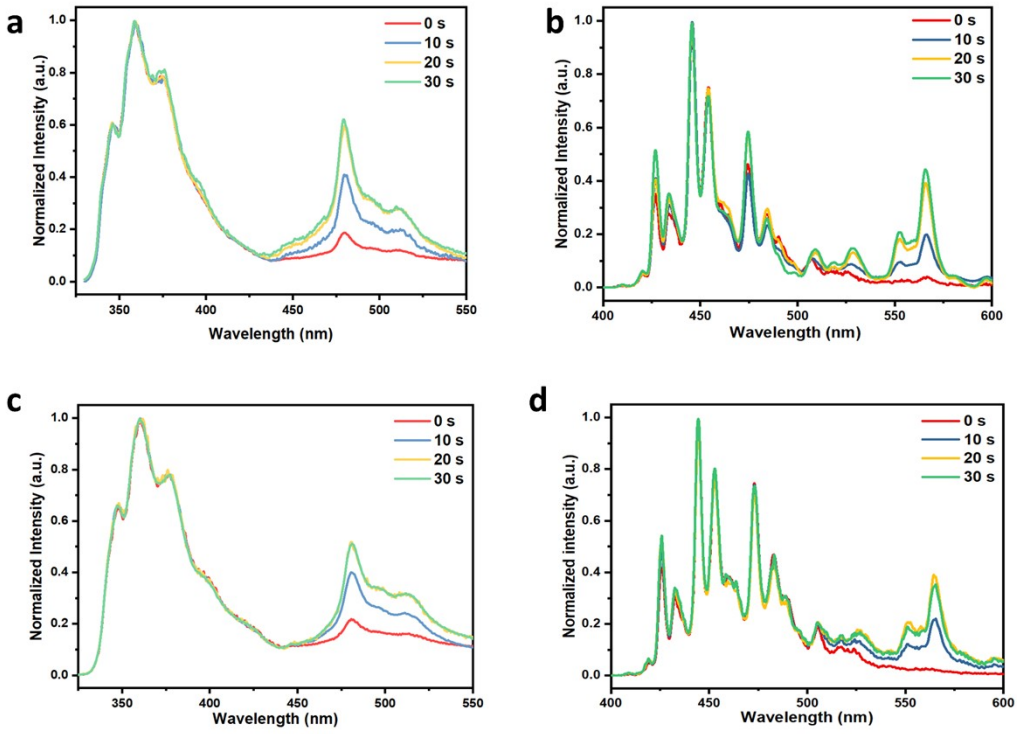

Fig. S18 The steady-state photoluminescence spectra for (a)T-PMMA, (b)C-PMMA,

(c)T-PC and (d)C-PC during the UV-irradiation process.

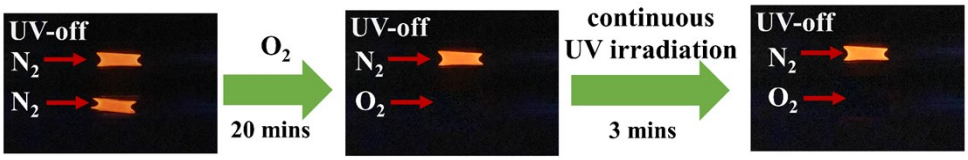

Fig. S19. Photographs of the H-PC exposed to O_2 and N_2 after turning off the UV irradiation.

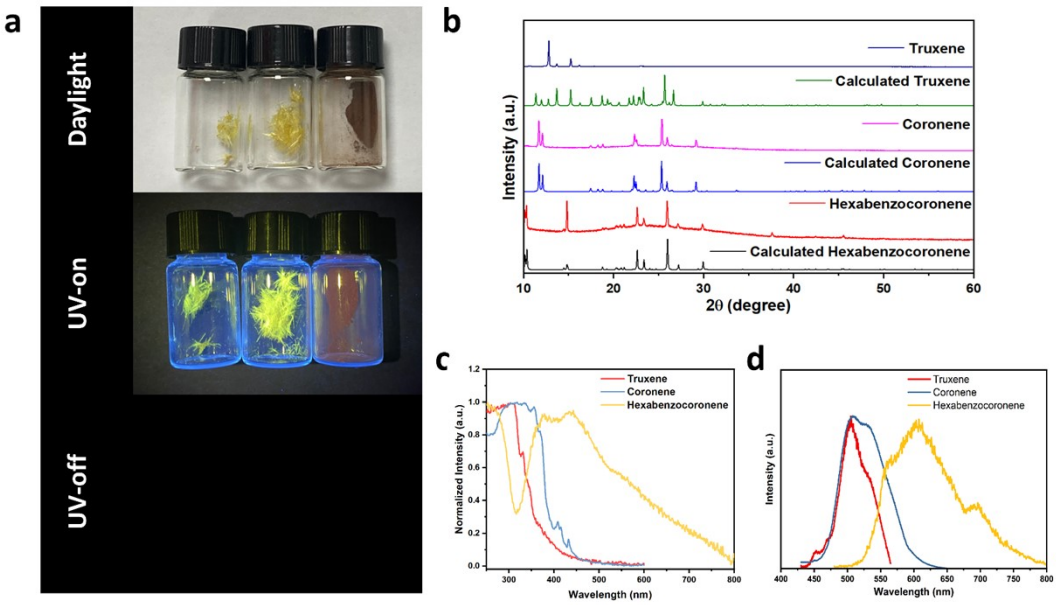

Fig. S20. (a) Photographs of the truxene, coronene and hexabenzocoronene crystals under the daylight, before and after turning off the excitation light. (b) The powder X-ray diffraction (PXRD) of truxene, coronene and hexabenzocoronene crystals. (c) The absorption spectra of truxene, coronene and hexabenzocoronene crystals. (d) The steady-state photoluminescence spectra of truxene, coronene and hexabenzocoronene crystals.

Table S3. Detailed Single-Crystal Structural Information of truxene, coronene and hexabenzocoronene crystals.

	Truxene	**Coronene**	**Hexabenzocoronene**
Empirical formula	$C_{27}H_{18}$	$C_{12}H_6$	$C_{42}H_{18}$
Formula weight	342.41	150.17	522.56
Temperature	300(2) K	293(2) K	
Wavelength	1.54178 Å	1.54184 Å	0.71073
Crystal system	Monoclinic	Monoclinic	Monoclinic
Space group	P 21/c	P 21/c	P 21/c

Unit cell dimensions	a = 4.8045(4) Å, b = 15.5425(15)Å, c = 23.249(2) Å, alpha = 90°, beta = 92.476(6)°, gamma = 90°.	a = 10.0981(5) Å, b = 4.6964(2) Å, c = 15.6980(10) Å alpha = 90°, beta = 106.070(6)°, gamma = 90°.	a=18.431(3), b=5.119(1), c=12.929(2), alpha =90°, beta =112.57(1) °, gamma =90°.
Volume	1734.5(3) $Å^3$	715.39(7) $Å^3$	1126.4 $Å^3$
Z	4	4	2
Density (calculated)	1.311 g/cm^3	1.394 g/cm^3	1.541 g/cm^3
Absorption coefficient	0.563 mm^{-1}	0.605 mm^{-1}	
F(000)	720	312	540
Crystal size	0.20 x 0.10 x 0.10 mm^3	0.03 x 0.03 x 0.02 mm^3	
Theta range for data collection	3.42 to 68.35°.	4.687 to 67.033°.	
Index ranges	-5<=h<=5, -13<=k<=18, -25<=l<=27	-12<=h<=12, -5<=k<=3, -16<=l<=18	
Reflections collected	12727	3718	
Independent reflections	3100 [R(int) = 0.0865]	1268 [R(int) = 0.0453]	
Completeness	97.40%	98.60%	
Absorption correction	Semi-empirical from equivalents	Semi-empirical from equivalents	
Max. and min. transmission	0.9459 and 0.8958	1.00000 and 0.93756	
Refinement method	Full-matrix least-squares on F2	Full-matrix least-squares on F2	
Data / restraints / parameters	3100 / 0 / 245	1268 / 0 / 110	
Goodness-of-fit on F^2	1.042	1.08	
Final R indices [I>2sigma(I)]	R1 = 0.0960, wR2 = 0.2701	R1 = 0.0635, wR2 = 0.1639	0.0560(0) 0.0560(0)
R indices (all data)	R1 = 0.1179, wR2 = 0.2875	R1 = 0.0762, wR2 = 0.1774	
Extinction coefficient	0.030(4)	0.014(3)	
Largest diff. peak and hole	0.415 and -0.296 $e.Å^{-3}$	0.306 and -0.255 $e.Å^{-3}$	
Data sources	Our work	Our work	Ref.[44]

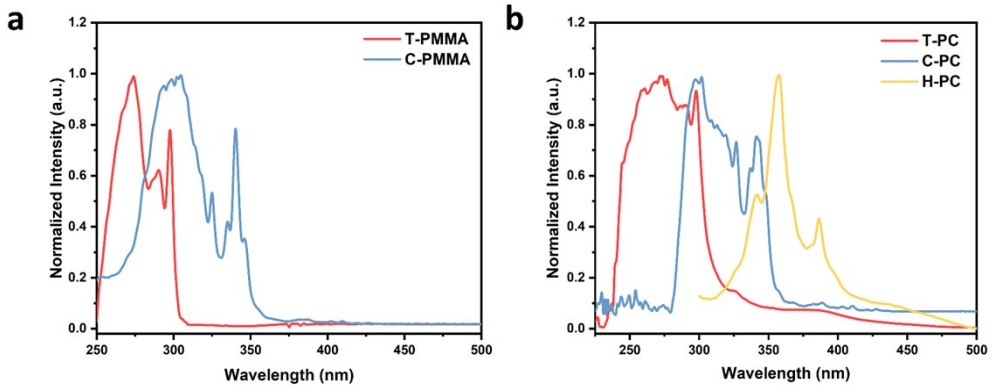

Fig. S21. (a) The absorption spectra of T-PMMA and C-PMMA. (b) The absorption spectra of T-PC, C-PC and H-PC.

Table S4. The singlet and triplet excited state transition configurations of isolated truxene revealed by TD-DFT calculations. The matched excited states that contain the same orbital transition components of S_1 and $|S_1-T_n| < 0.3$ eV were highlighted in red.

Truxene			
Singlet excited state	**Triplet excited state**	**Energy**	**Transition configuration (%)**
S_1 3.9590 eV, H -> L 55.3%, H-1 -> L+1 32.9%, H -> L+1 5.3%	**T_1**	**2.6210 eV**	**H -> L+1 37.3%, H-1 -> L 31.4%, H -> L 7.3%, H-1 -> L+1 5.4%**
	T_2	**3.1680 eV**	**H -> L 26.0%, H-1 -> L+1 17.2%, H-1 -> L 5.9%, H-2 -> L+1 5.3%**
	T_3	**3.2110 eV**	**H-1 -> L 24.5%, H -> L+1 22.7%, H -> L 5.7%, H-2 -> L 5.1%**
	T_4	**3.7090 eV**	**H -> L 41.9%, H -> L+1 13.5%, H-1 -> L+3 5.2%**
	T_5	**3.7530 eV**	**H-1 -> L+1 16.1%, H-1 -> L 11.6%, H-2 -> L+2 7.7%, H-3 -> L+5 5.7%, H -> L+1 5.4%, H-2 -> L+1 5.1%**
	T_6	**3.8170 eV**	**H-1 -> L+1 25.1%, H-1 -> L 12.9%, H -> L 10.9%, H-4 -> L+4 6.7%**
	T_7	**3.8680 eV**	**H-1 -> L+1 24.4%, H -> L+1 6.8%, H-5 -> L+2 5.9%, H-2 -> L+2 5.8%, H-4 -> L+5 5.5%**
	T_8	**4.2230 eV**	**H -> L+2 19.8%, H -> L+4 14.2%, H -> L+5 12.4%, H -> L+3 10.2%, H-5 -> L+1 5.5%**
	T_9	**4.2530 eV**	**H-1 -> L+2 14.1%, H-2 -> L+1 10.7%, H -> L+4 10.5%, H-5 -> L 7.9%, H-3 -> L 6.8%, H-2 -> L 6.4%, H-3 -> L+3 5.4%, H-3 -> L+1 5.4%**
	T_{10}	**4.2990 eV**	**H-1 -> L+3 13.8%, H-1 -> L+2 11.8%, H-2 -> L 11.1%, H -> L+5 7.3%, H-1 -> L+5 7.3%, H-2 -> L+5 6.1%, H-3 -> L**

			5.5%

Table S5. The singlet and triplet excited state transition configurations of isolated coronene revealed by TD-DFT calculations. The matched excited states that contain the same orbital transition components of S_1 and $|S_1-T_n| < 0.3$ eV were highlighted in red.

Coronene			
Singlet excited state	**Triplet excited state**	**Energy**	**Transition configuration (%)**
S_1 3.3070 eV, H-1 -> L 26.7%, H -> L+1 26.7%, H -> L 22.8%, H-1 -> L+1 22.8%	T_1	2.1810 eV	H -> L 23.0%, H-1 -> L+1 23.0%, H-1 -> L 19.7%, H -> L+1 19.7%
	T_2	3.0110 eV	H -> L+1 41.6%, H-1 -> L 41.6%, H-1 -> L+1 6.9%, H -> L 6.9%
	T_3	3.0110 eV	H-1 -> L+1 41.6%, H -> L 41.5%, H-1 -> L 6.9%, H -> L+1 6.9%
	T_4	3.1580 eV	H -> L+1 26.6%, H-1 -> L 26.5%, H -> L 22.7%, H-1 -> L+1 22.6%
	T_5	3.5170 eV	H -> L+3 15.6%, H-1 -> L+2 15.5%, H-3 -> L 8.3%, H-2 -> L+1 8.3%, H-5 -> L+1 7.2%, H-1 -> L+4 7.1%, H -> L+5 6.5%, H-4 -> L 5.5%
	T_6	3.5180 eV	H-1 -> L+3 15.6%, H -> L+2 15.6%, H-2 -> L 8.3%, H-3 -> L+1 8.3%, H-5 -> L 7.2%, H -> L+4 7.0%, H-1 -> L+5 6.5%, H-4 -> L+1 5.4%
	T_7	3.7640 eV	H-2 -> L 17.3%, H-3 -> L+1 17.2%, H-1 -> L+3 16.1%, H -> L+2 16.0%, H-1 -> L+2 12.8%, H -> L+3 12.7%
	T_8	4.0600 eV	H -> L+3 20.1%, H-1 -> L+2 20.1%, H -> L+2 16.0%, H-1 -> L+3 16.0%, H-3 -> L 12.4%, H-2 -> L+1 12.4%
	T_9	4.3020 eV	H-1 -> L+4 38.2%, H-5 -> L+1 15.4%, H-4 -> L 14.1%, H -> L+5 9.0%, H-5 -> L 5.9%, H-4 -> L+1 5.4%
	T_{10}	4.3020 eV	H -> L+4 38.2%, H-5 -> L 15.5%, H-4 -> L+1 14.1%, H-1 -> L+5 9.1%, H-5 -> L+1 6.0%, H-4 -> L 5.4%

Table S6. The singlet and triplet excited state transition configurations of isolated hexabenzocoronene revealed by TD-DFT calculations. The matched excited states that contain the same orbital transition components of S_1 and $|S_1-T_n| < 0.3$ eV were highlighted in red.

Hexabenzocoronene			
Singlet excited state	**Triplet excited**	**Energy**	**Transition configuration (%)**

	state		
S_1 2.9850 eV, H-1 -> L 49.1%, H -> L+1 49.1%	T_1	1.9600 eV	H -> L 33.7%, H-1 -> L+1 33.7%, H-2 -> L+2 18.6%
	T_2	2.5180 eV	H-1 -> L+2 30.3%, H-2 -> L+1 18.9%, H -> L+2 16.7%, H-2 -> L 9.2%
	T_3	2.5180 eV	H -> L+2 30.3%, H-2 -> L 18.9%, H-1 -> L+2 16.7%, H-2 -> L+1 9.2%
	T_4	2.7820 eV	H -> L+1 32.4%, H-1 -> L 32.3%, H -> L 15.5%, H-1 -> L+1 15.5%
	T_5	2.7820 eV	H-1 -> L+1 32.3%, H -> L 32.3%, H-1 -> L 15.5%, H -> L+1 15.5%
	T_6	2.8900 eV	H-1 -> L 48.4%, H -> L+1 48.4%
	T_7	3.1050 eV	H-2 -> L+2 43.7%, H -> L+4 11.3%, H-1 -> L+5 11.2%, H-1 -> L+1 7.3%, H -> L 7.3%, H-4 -> L 7.1%, H-5 -> L+1 7.1%
	T_8	3.3580 eV	H -> L+3 18.2%, H-1 -> L+4 13.9%, H -> L+5 13.9%, H-3 -> L 8.0%, H-4 -> L+1 8.0%, H-5 -> L 7.9%, H-6 -> L+2 5.7%
	T_9	3.3580 eV	H-1 -> L+3 18.1%, H-1 -> L+5 14.0%, H -> L+4 13.9%, H-3 -> L+1 8.0%, H-5 -> L+1 8.0%, H-4 -> L 7.9%, H-7 -> L+2 5.7%
	T_{10}	3.3960 eV	H-2 -> L 46.1%, H -> L+2 42.8%

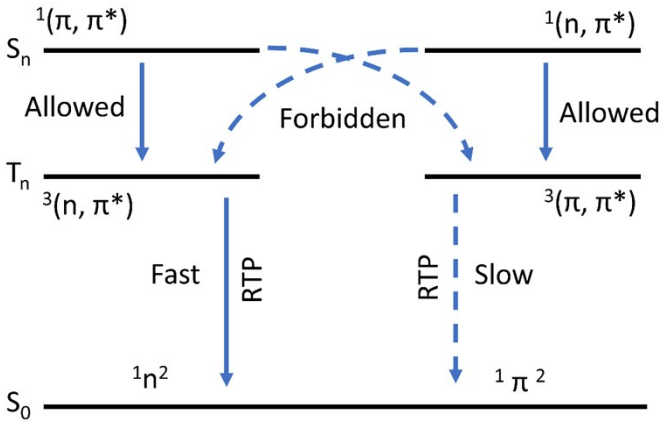

Fig. S22. EI-Sayed rule in organic luminescence materials.

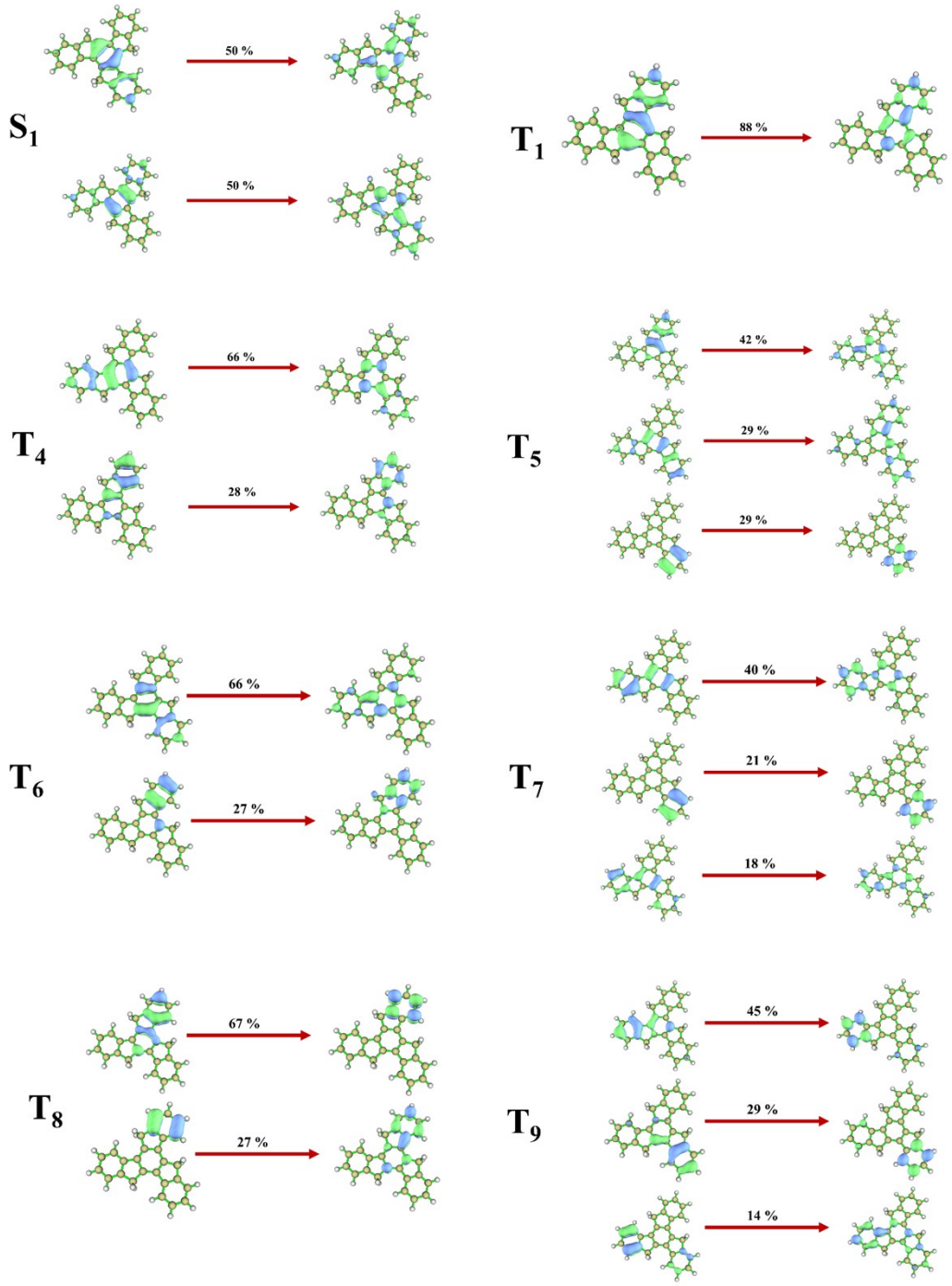

Fig. S23. Hole and particle pairs in natural transition orbitals (NTOs) analysis for $S_0 \rightarrow S_1$ and $S_0 \rightarrow T_n$ transitions of truxene. (The energy level of a triplet state (T_n) lies within the range of ± 0.3 eV to E_{S1})

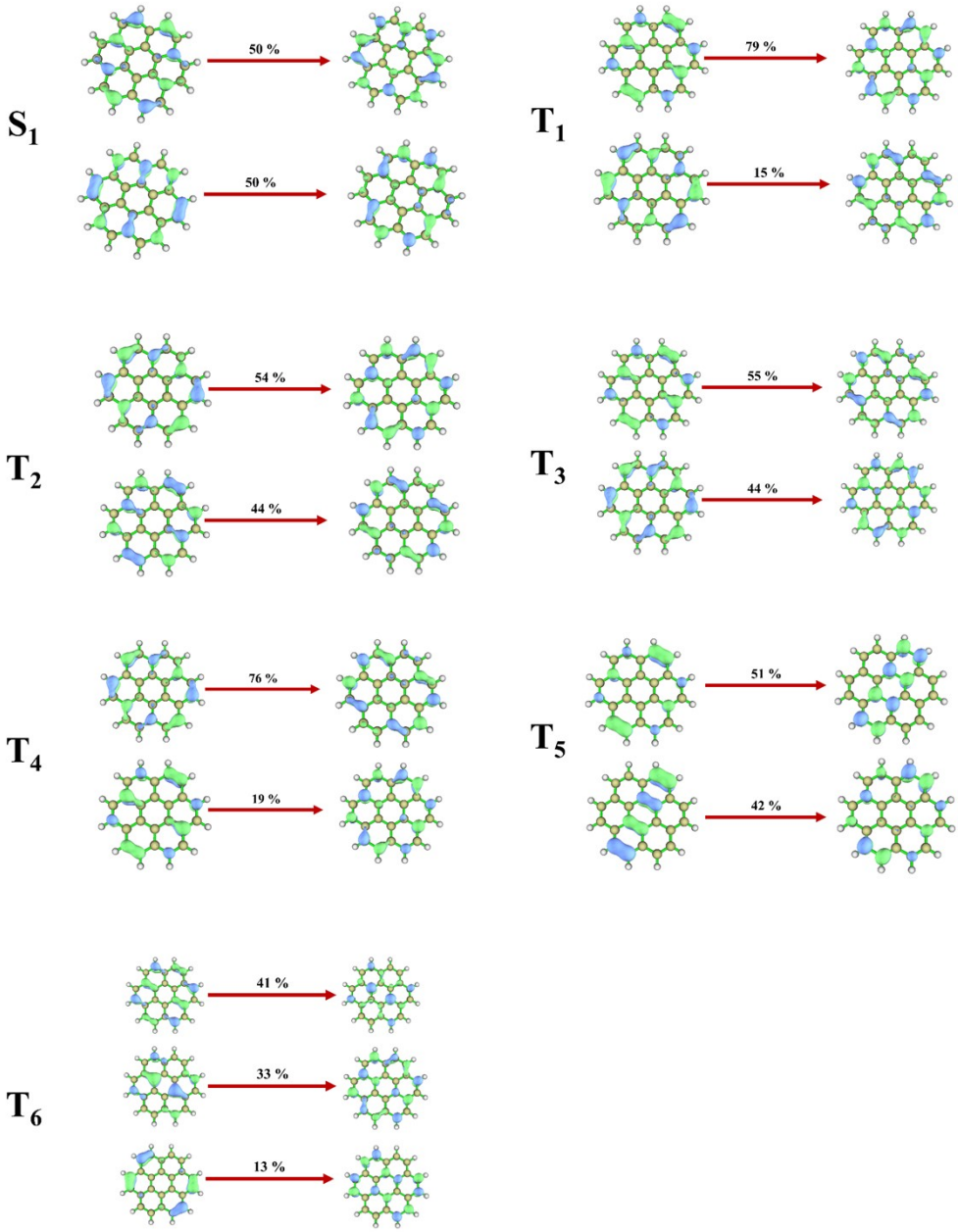

Fig. S24. Hole and particle pairs in natural transition orbitals (NTOs) analysis for $S_0 \rightarrow S_1$ and $S_0 \rightarrow T_n$ transitions of coronene. (The energy level of a triplet state (T_n)

lies within the range of ± 0.3 eV to E_{S1})

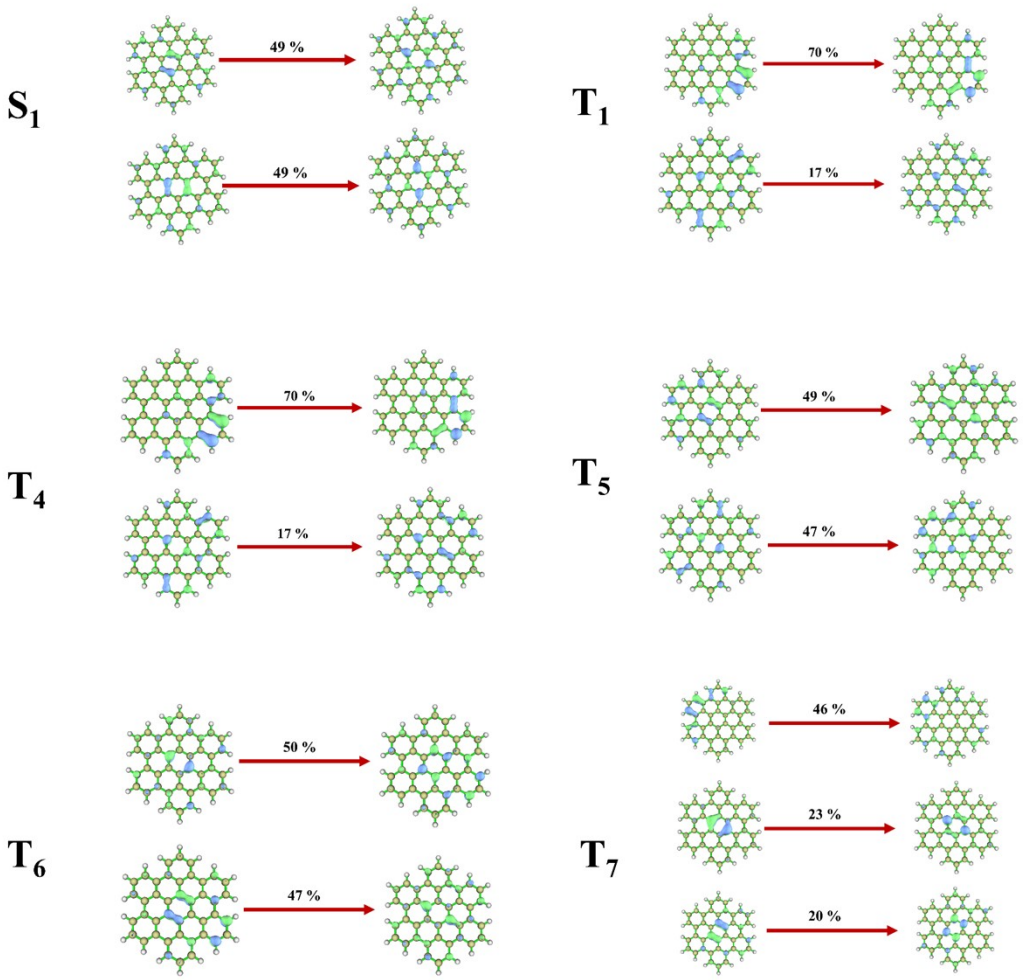

Fig. S25. Hole and particle pairs in natural transition orbitals (NTOs) analysis for $S_0 \rightarrow S_1$ and $S_0 \rightarrow T_n$ transitions of hexabenzocoronene. (The energy level of a triplet state (T_n) lies within the range of ± 0.3 eV to E_{S1})

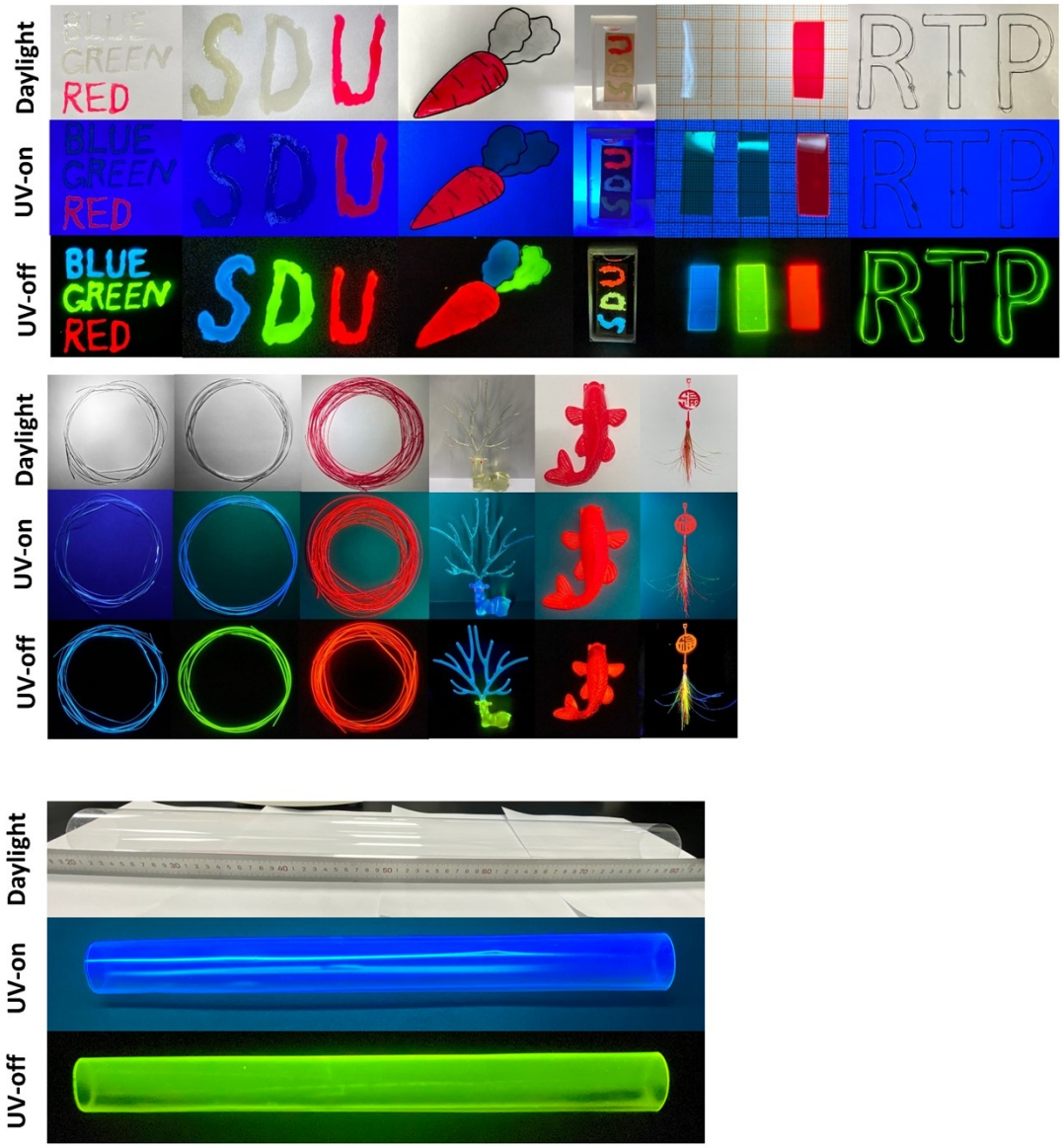

Fig. S26. Detailed photographs of various forms of PMMA-based RTP materials for sundry application situations.

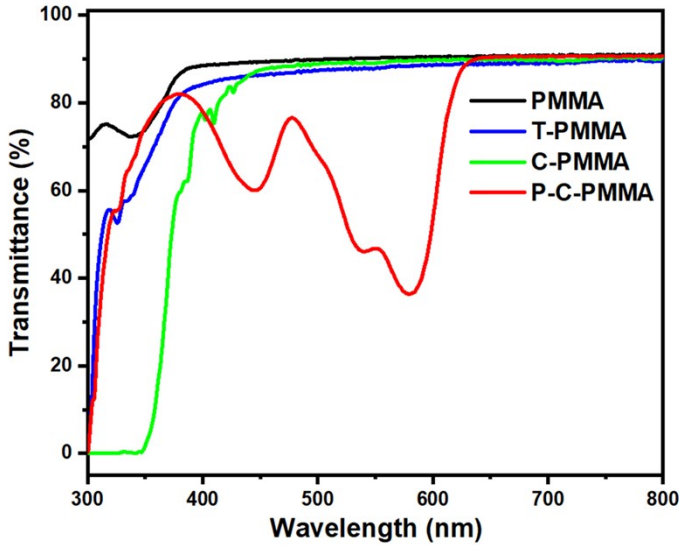

Fig. S27. Transmission of a pure PMMA film and T-PMMA, C-PMMA, and P-PMMA films. Their thicknesses were all about 0.6 mm.

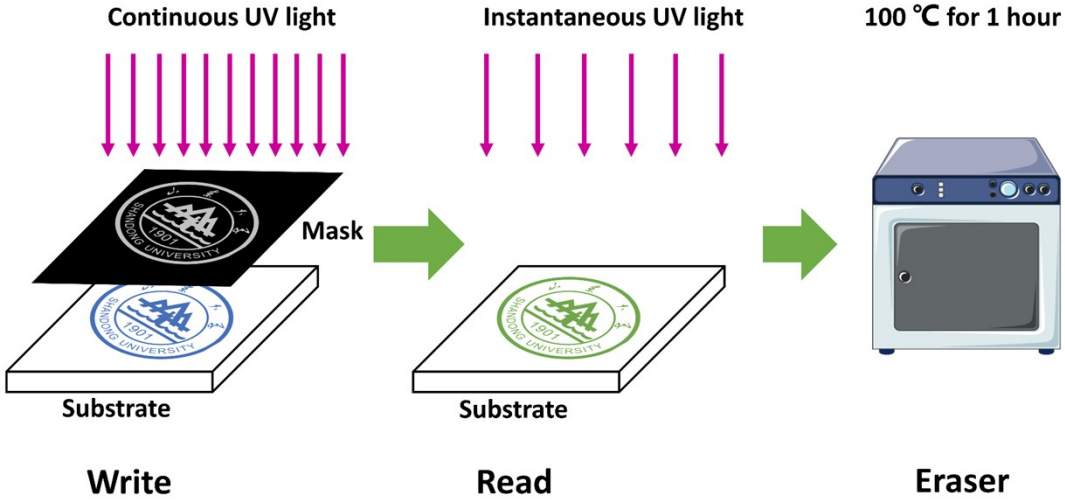

Fig. S28. Overview of writing, reading and erasing procedure based on RTP films. Writing: Masked UV illumination used for the pattern of the emblem of Shandong University. Reading: High luminescent contrast is achieved by phosphorescence on mask-illuminated areas in delayed emission. Erasing: By heating the sample for around 1 hour at 100 ℃.

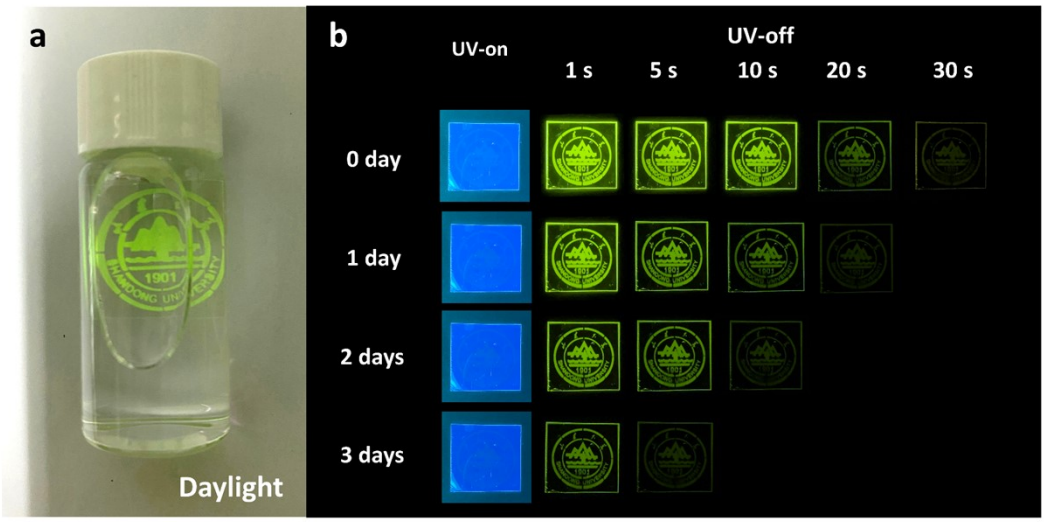

Fig. S29. (a) Photographs of the written afterglow patterns, in which the display of high-brightness RTP images could be achieved even in daylight. (b) Photographs of the changes in written afterglow patterns over time.

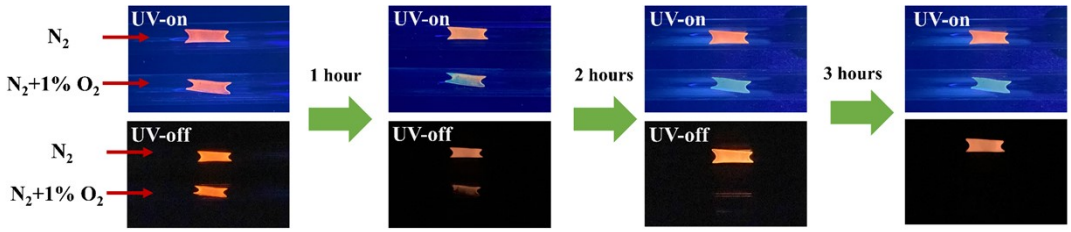

Fig. S30. Photographs of the H-PC oxygen monitor exposed to pure and 1% (v/v) O_2 containing N_2 under UV irradiation and after turning off the UV irradiation.

References

[1] F. Tian Lu, *Journal of Computational Chemistry* **2012**, 33, 580.

[2] a)F. Neese, *Wiley Interdiscip. Rev.: Comput. Mol. Sci.* **2012**, 2, 73; b)F. Neese, *Wiley Interdisciplinary Reviews: Computational Molecular Science* **2018**, 8, e1327.

[3] W. Humphrey, A. Dalke, K. Schulten, *Journal of molecular graphics* **1996**, 14, 33.

[4] a)R. Sharma, M. B. Thomas, R. Misra, F. D'Souza, *Angew Chem Int Ed Engl* **2019**, 58, 4350; b)J. Cao, Y. M. Liu, X. Jing, J. Yin, J. Li, B. Xu, Y. Z. Tan, N. Zheng, *J Am Chem Soc* **2015**, 137, 10914.

[5] S. Reineke, N. Seidler, S. R. Yost, F. Prins, W. A. Tisdale, M. A. Baldo, *Applied Physics Letters* **2013**, 103.

[6] X. Chen, C. Xu, T. Wang, C. Zhou, J. Du, Z. Wang, H. Xu, T. Xie, G. Bi, J. Jiang, *Angewandte Chemie International Edition* **2016**, 55, 9872.

[7] a)H. Mieno, R. Kabe, N. Notsuka, M. D. Allendorf, C. Adachi, *Advanced Optical Materials* **2016**, 4, 1015; b)J. L. Kropp, W. R. Dawson, *The Journal of Physical Chemistry* **1967**, 71, 4499; c)M. Wu, X. Wang, Y. Pan, J. Li, X. Li, Y. Sun, Y. Zou, H. Zhang, K. Zhang, *The Journal of Physical Chemistry C* **2021**, 125, 26986.

[8] M. Louis, H. Thomas, M. Gmelch, A. Haft, F. Fries, S. Reineke, *Adv Mater* **2019**, 31, e1807887.

[9] F. Fries, M. Louis, R. Scholz, M. Gmelch, H. Thomas, A. Haft, S. Reineke, *J Phys Chem A* **2020**, 124, 479.

[10] H. Thomas, D. L. Pastoetter, M. Gmelch, T. Achenbach, A. Schlogl, M. Louis, X. Feng, S. Reineke, *Adv Mater* **2020**, 32, e2000880.

[11] M. Louis, H. Thomas, M. Gmelch, F. Fries, A. Haft, J. Lindenthal, S. Reineke, *Advanced Optical Materials* **2020**, 8.

[12] S. Xu, R. E. Evans, T. Liu, G. Zhang, J. N. Demas, C. O. Trindle, C. L. Fraser, *Inorg Chem* **2013**, 52, 3597.

[13] M. L. Daly, C. Kerr, C. A. DeRosa, C. L. Fraser, *ACS Appl Mater Interfaces* **2017**, 9, 32008.

[14] T. Liu, G. Zhang, R. E. Evans, C. O. Trindle, Z. Altun, C. A. DeRosa, F. Wang, M. Zhuang, C. L. Fraser, *Chemistry* **2018**, 24, 1859.

[15] M. Kolpaczynska, C. A. DeRosa, W. A. Morris, C. L. Fraser, *Australian journal of chemistry* **2016**, 69, 537.

[16] C. A. DeRosa, M. L. Daly, C. Kerr, C. L. Fraser, *ChemPhotoChem* **2018**, 3, 31.

[17] R. Gao, X. Fang, D. Yan, *Journal of Materials Chemistry C* **2018**, 6, 4444.

[18] H. Wu, W. Chi, Z. Chen, G. Liu, L. Gu, A. K. Bindra, G. Yang, X. Liu, Y. Zhao, *Advanced Functional Materials* **2019**, 29.

[19] H. Wu, L. Gu, G. V. Baryshnikov, H. Wang, B. F. Minaev, H. Agren, Y. Zhao, *ACS Appl Mater Interfaces* **2020**, 12, 20765.

[20] a)S. Kuila, S. J. George, *Angew Chem Int Ed Engl* **2020**, 59, 9393; b)S. Kuila, S. Garain, S. Bandi, S. J. George, *Advanced Functional Materials* **2020**, 30.

[21] Y. Su, S. Z. F. Phua, Y. Li, X. Zhou, D. Jana, G. Liu, W. Q. Lim, W. K. Ong, C. Yang, Y. Zhao, *Science advances* **2018**, 4, eaas9732.

[22] Y. Zhang, L. Gao, X. Zheng, Z. Wang, C. Yang, H. Tang, L. Qu, Y. Li, Y. Zhao, *Nat Commun* **2021**, 12, 2297.

[23] Y. Su, Y. Zhang, Z. Wang, W. Gao, P. Jia, D. Zhang, C. Yang, Y. Li, Y. Zhao, *Angew Chem Int Ed Engl* **2020**, 59, 9967.

[24] Z. Wang, Y. Zhang, C. Wang, X. Zheng, Y. Zheng, L. Gao, C. Yang, Y. Li, L. Qu, Y. Zhao, *Adv Mater* **2020**, 32, e1907355.
[25] H. Wu, D. Wang, Z. Zhao, D. Wang, Y. Xiong, B. Z. Tang, *Advanced Functional Materials* **2021**, 31.
[26] Y. Yang, Y. Liang, Y. Zheng, J. A. Li, S. Wu, H. Zhang, T. Huang, S. Luo, C. Liu, G. Shi, F. Sun, Z. Chi, B. Xu, *Angew Chem Int Ed Engl* **2022**.
[27] Z. Wang, L. Gao, Y. Zheng, Y. Zhu, Y. Zhang, X. Zheng, C. Wang, Y. Li, Y. Zhao, C. Yang, *Angew Chem Int Ed Engl* **2022**.
[28] W. Tao, Y. Zhou, F. Lin, H. Gao, Z. Chi, G. Liang, *Advanced Optical Materials* **2022**.
[29] Y. Zhang, Y. Su, H. Wu, Z. Wang, C. Wang, Y. Zheng, X. Zheng, L. Gao, Q. Zhou, Y. Yang, X. Chen, C. Yang, Y. Zhao, *J Am Chem Soc* **2021**, 143, 13675.
[30] Y. Yang, J. Wang, D. Li, J. Yang, M. Fang, Z. Li, *Adv Mater* **2021**, e2104002.
[31] Y. Li, L. Jiang, W. Liu, S. Xu, T. Y. Li, F. Fries, O. Zeika, Y. Zou, C. Ramanan, S. Lenk, R. Scholz, D. Andrienko, X. Feng, K. Leo, S. Reineke, *Adv Mater* **2021**, e2101844.
[32] R. Chen, Y. Guan, H. Wang, Y. Zhu, X. Tan, P. Wang, X. Wang, X. Fan, H. L. Xie, *ACS Appl Mater Interfaces* **2021**, 13, 41131.
[33] a)M. Gmelch, H. Thomas, F. Fries, S. Reineke, *Science advances* **2019**, 5, eaau7310; b)A. Kirch, M. Gmelch, S. Reineke, *J Phys Chem Lett* **2019**, 10, 310.
[34] F. Lin, H. Wang, Y. Cao, R. Yu, G. Liang, H. Huang, Y. Mu, Z. Yang, Z. Chi, *Adv Mater* **2022**, e2108333.
[35] D. Li, Y. Yang, J. Yang, M. Fang, B. Z. Tang, Z. Li, *Nat Commun* **2022**, 13, 347.
[36] Y. Zhu, Y. Guan, Y. Niu, P. Wang, R. Chen, Y. Wang, P. Wang, H. L. Xie, *Advanced Optical Materials* **2021**, 9.
[37] B. Zhao, S. Yang, X. Yong, J. Deng, *ACS Appl Mater Interfaces* **2021**, 13, 59320.
[38] S. Cai, H. Ma, H. Shi, H. Wang, X. Wang, L. Xiao, W. Ye, K. Huang, X. Cao, N. Gan, C. Ma, M. Gu, L. Song, H. Xu, Y. Tao, C. Zhang, W. Yao, Z. An, W. Huang, *Nat Commun* **2019**, 10, 4247.
[39] T. Ogoshi, H. Tsuchida, T. Kakuta, T. a. Yamagishi, A. Taema, T. Ono, M. Sugimoto, M. Mizuno, *Advanced Functional Materials* **2018**, 28.
[40] a)G. Zhang, J. Chen, S. J. Payne, S. E. Kooi, J. Demas, C. L. Fraser, *Journal of the American Chemical Society* **2007**, 129, 8942; b)G. Zhang, G. M. Palmer, M. W. Dewhirst, C. L. Fraser, *Nat Mater* **2009**, 8, 747.
[41] L. Gu, H. Wu, H. Ma, W. Ye, W. Jia, H. Wang, H. Chen, N. Zhang, D. Wang, C. Qian, Z. An, W. Huang, Y. Zhao, *Nat Commun* **2020**, 11, 944.
[42] X. Dou, T. Zhu, Z. Wang, W. Sun, Y. Lai, K. Sui, Y. Tan, Y. Zhang, W. Z. Yuan, *Adv Mater* **2020**, 32, e2004768.
[43] H. Peng, G. Xie, Y. Cao, L. Zhang, X. Yan, X. Zhang, S. Miao, Y. Tao, H. Li, C. Zheng, *Science advances* **2022**, 8, eabk2925.
[44] R. Goddard, M. W. Haenel, W. C. Herndon, C. Krueger, M. Zander, *Journal of the American Chemical Society* **1995**, 117, 30.